西安電子科技大學
XIDIAN UNIVERSITY

Wideband Interference Mitigation for Synthetic Aperture Radar Based on Variational Bayesian Inference

Yi Ding, Weiwei Fan, and Feng Zhou*

August 19th, 2020

Key Laboratory of electronic information countermeasure and simulation technology of ministry of education,
Xidian University, Xi'an, China

Outline

- **Motivation**
- **Signal modeling and time-frequency (TF) analysis**
  - **Low-rank characteristics of WBI in TF domain**
  - **Statistical characteristics of the signal**
- **WBI mitigation methodology**
  - **Bayesian model formulation**
  - **Approximate variational Bayesian inference**
- **Experimental results**
- **Conclusion remarks**

Motivation - Wide application of SAR

- Urban construction planning

- Ship detection

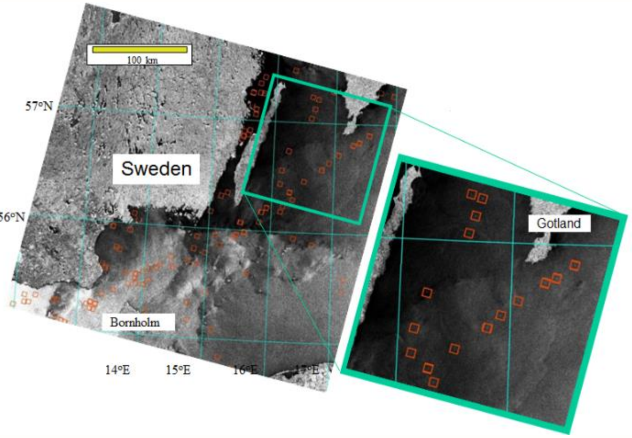

- Disaster monitoring

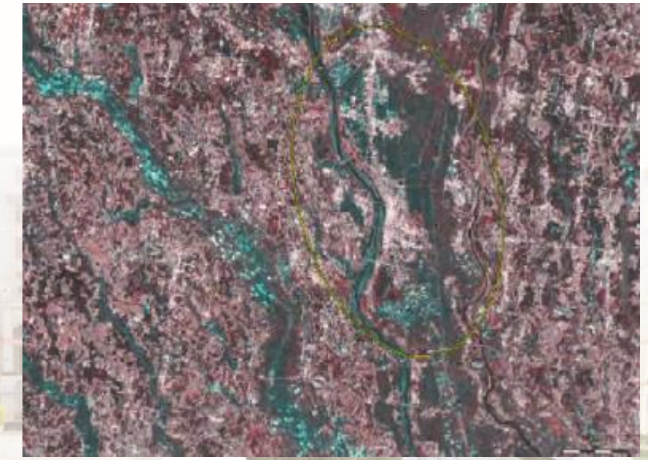

- Vegetation coverage survey

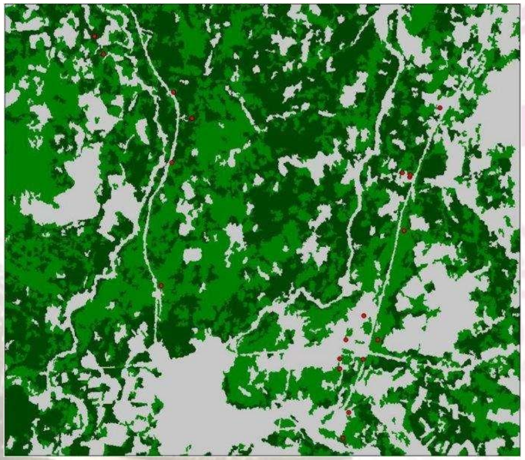

Motivation - Radio Frequency Interference (RFI)

- **Radio frequency band become very crowded**

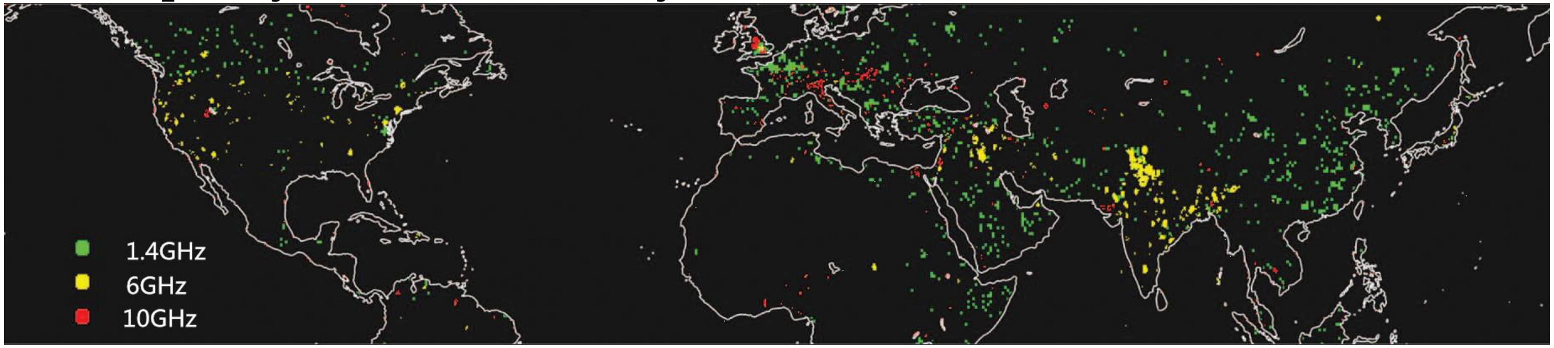

- **Complex radio environment**

- **SAR is more likely to contaminate by RFI for its wide frequency band**

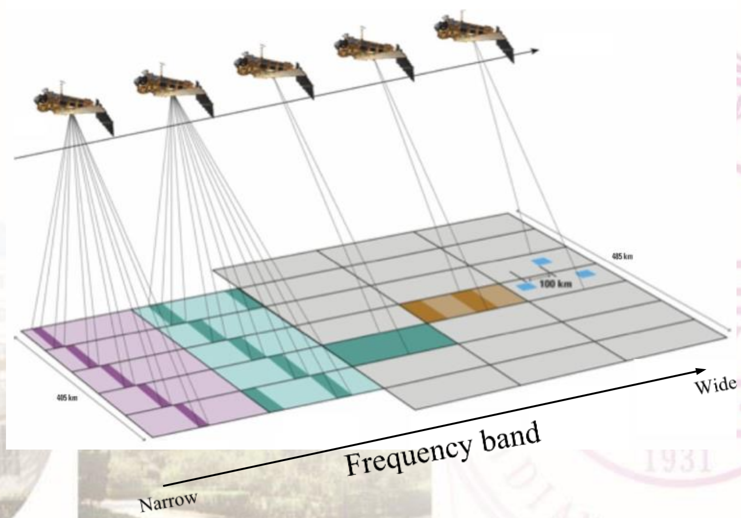

Motivation - Adverse impacts of RFI

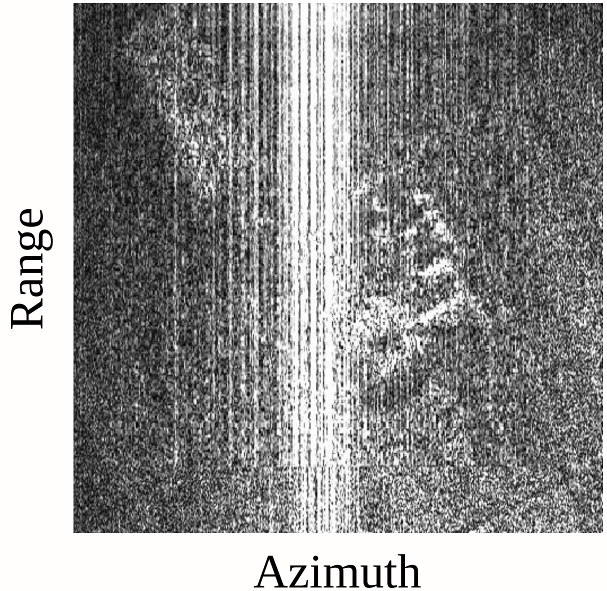

SAR image corrupted with NBI

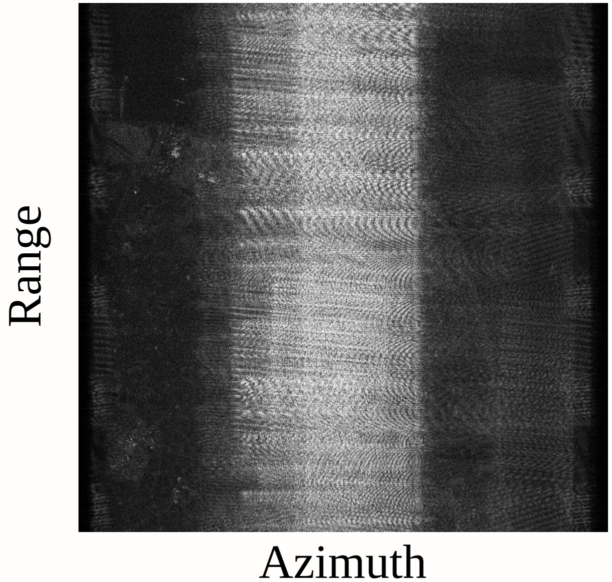

SAR image corrupted with WBI

RFI have intuitive adverse impacts on SAR imaging.

- RFI would reduce signal-to-interference-plus-noise power ratio (SINR) of SAR data
- RFI would yield inaccurate estimates of critical Doppler parameters
- RFI would abate the accuracy of feature extraction and posing a hindrance to the SAR image interpretation

It is necessary to develop interference mitigation method for SAR.

Motivation - Research status

SAR RFI mitigation techniques are divided into data-driven algorithms and model-driven algorithms.

Data-driven algorithms

- design a reasonable filter
- separate the interference and useful signal in a specific domain

Deficiency :

- Large loss of signal energy
- Dependent on the quantity and quality of interference samples (as for deep learning algorithms)

Model-driven algorithms

- utilize mathematical models to characterize the SAR echoes
- optimize the model parameters under specific criteria

Deficiency :

- Heavy calculation burden
- The poor mitigation result due to the inaccuracy signal model
- The lack of robustness for different scenes

Signal modeling and TF analysis

- SAR received echo model

$$s(k) = x(k) + i(k) + n(k)$$

- WBI -- $i(k): CMWBI, SMWBI$
- SAR echo -- $s(k)$
- Radar system noise -- $n(k)$

- The simplified signal model
  - ➢ The energy of effective interference is much greater than that of target signal.
  - ➢ Compared with the strong WBI, the target signal has a noise-like distribution.

Assumption → noise-like distribution →

$$s(k) = i(k) + n_x(k)$$

- The equivalent additive noise -- $n_x(k)$: $n_x(k) = n(k) + x(k)$

Signal modeling and TF analysis

- The signal characteristics of time and frequency domain is not incomplete.
- Radar echo is time-varying nonstationary signal.
- STFT tools could provide time-localized spectral information of the frequency components of a signal varying over time

$$STFT_y(\tau, f) = \int_{-\infty}^{\infty} y(t) h(t-\tau) e^{-j2\pi ft} dt \Longleftrightarrow y(t) = \int_{-\infty}^{\infty}\int_{-\infty}^{\infty} STFT_y(\tau, f) w(t-\tau) e^{j2\pi ft} d\tau df$$

STFT is a linear invertible transformation.

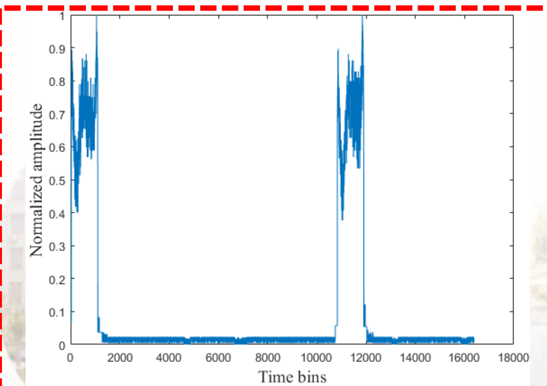

Time domain

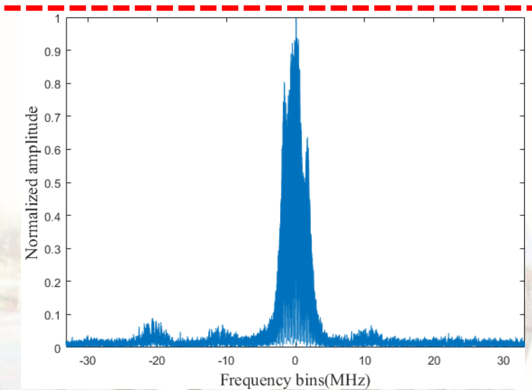

Frequency domain

STFT

ISTFT

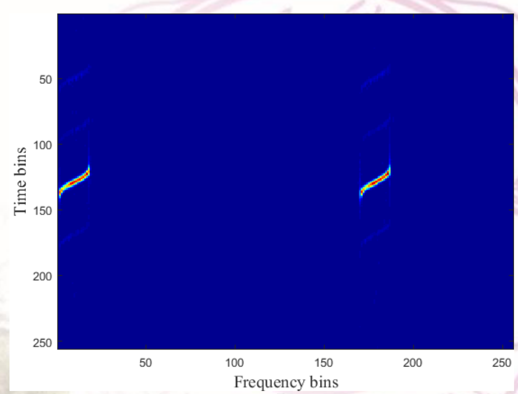

TF domain

Signal modeling and TF analysis

- The representation of SAR echo in TF domain

$$s(k) = i(k) + n_x(k)$$

STFT ⇕ ISTFT

$$\mathbf{S} = \mathbf{I} + \mathbf{N}$$

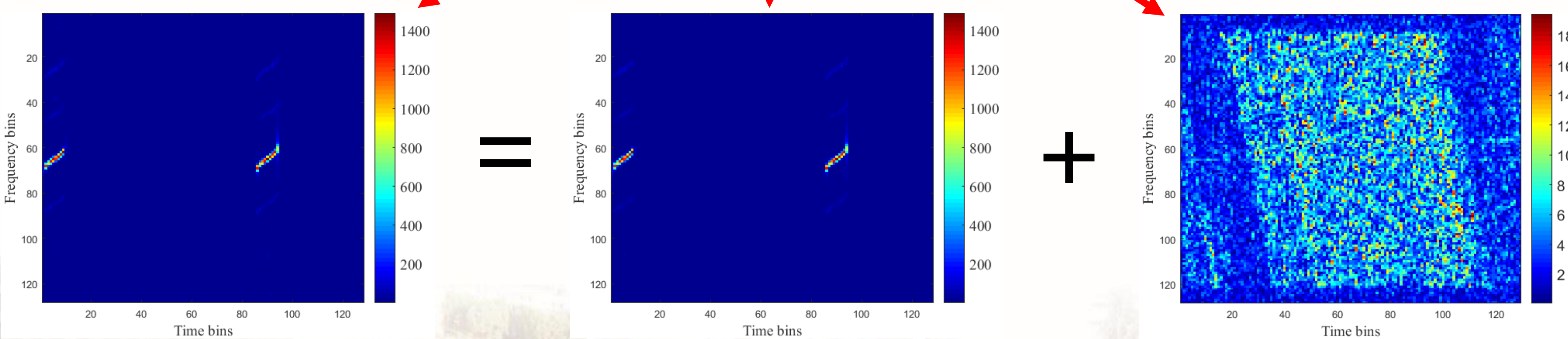

Our purpose is to separate target signal and interference in TF domain.

Signal modeling and TF analysis

- Low-rank characteristics of WBI in TF domain

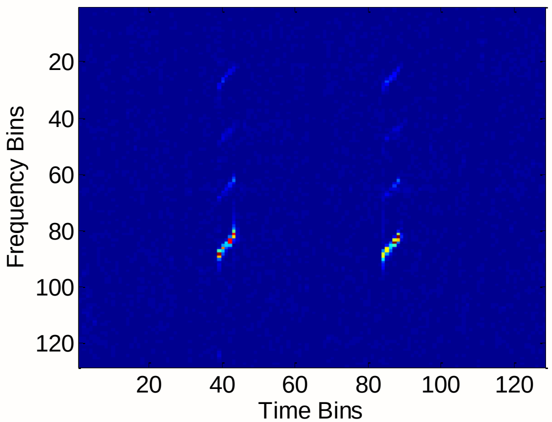

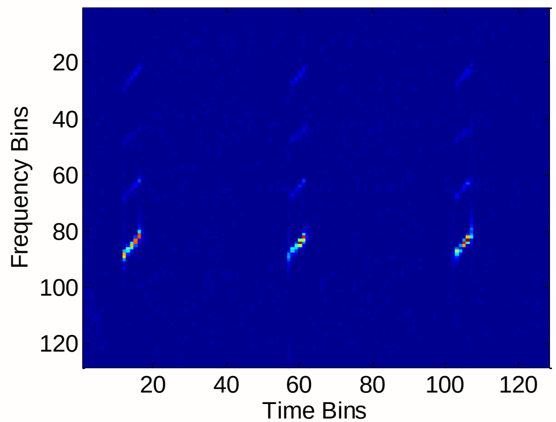

Different azimuth echoes from the measured WBI data

- Obviously, WBI only occupies a limited part in the TF domain.
- WBI is low-rank compared to the echo signal in the TF domain.

Low-rank matrix recovery

$$\min_{\mathbf{I}} \|\mathbf{S}-\mathbf{I}\|_p$$

Matrix factorization

$$\mathbf{I} = \mathbf{U}^H \mathbf{V}$$

Low-rank matrix factorization

$$\min_{\mathbf{U},\mathbf{V}} \|\mathbf{S}-\mathbf{U}^H\mathbf{V}\|_p$$

Signal modeling and TF analysis

- Statistical characteristics of the signal

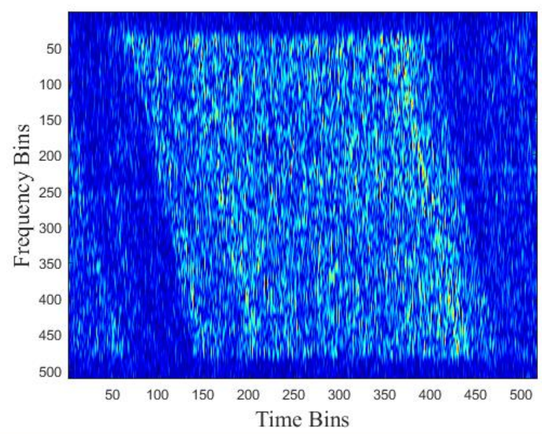

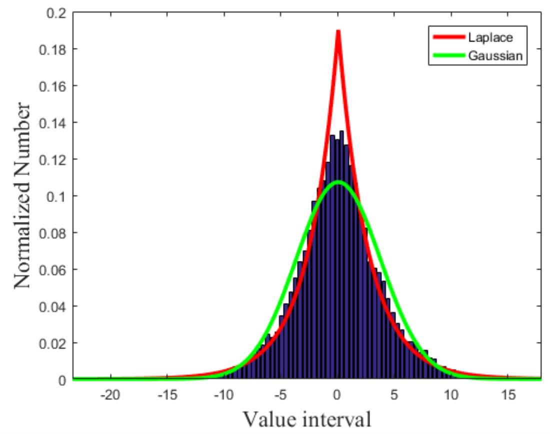

- ➢ Gaussian distribution hypothesis is used in traditional algorithms, which means L_2-norm optimization.
- ➢ It is sensitive to non-Gaussian noise and outlier value.
- ➢ The probability density of this data is more consistent with the Laplace distribution.

$$
\begin{aligned}
& l(\mathbf{S},\mathbf{I}) \\
& = -\prod_{(i,j)\in\Omega} \ln p\left(\mathbf{S}-\mathbf{I}\middle|0,b\right) \\
& = -\frac{1}{b}\left\|\mathbf{S}-\mathbf{I}\right\|_1 + C
\end{aligned}
$$

Low-rank matrix factorization $\min\limits_{\mathbf{U},\mathbf{V}} \left\|\mathbf{S}-\mathbf{U}^H\mathbf{V}\right\|_p$

Laplace distribution assumption

Low-rank matrix factorization $\min\limits_{\mathbf{U},\mathbf{V}} \left\|\mathbf{S}-\mathbf{U}^{\mathbf{H}}\mathbf{V}\right\|_1$

WBI mitigation methodology

- Bayesian model formulation
  - The TF noise has a Laplace distribution hypothesis, based on the previous analysis

$$p\left(\mathbf{N}_{ij}\middle|0,\sqrt{\frac{\lambda}{2}}\right)=\text{Laplace}\left(\mathbf{N}_{ij}\middle|0,\sqrt{\frac{\lambda}{2}}\right)$$
$$=\int_0^\infty CN\left(\mathbf{N}_{ij}\middle|0,z_{ij}\right)\text{Exponential}\left(z_{ij}\middle|\lambda\right)dz_{ij}$$

  - In general, we assume $\mathbf{u}_i$ and $\mathbf{v}_j$ obey the complex Gaussian-Gamma distribution

$$\mathbf{u}_i\sim CN\left(\mathbf{0},\tau_{u_i}^{-1}\mathbf{I}\right)\qquad \mathbf{v}_j\sim CN\left(\mathbf{0},\tau_{v_i}^{-1}\mathbf{I}\right)$$
$$\tau_{u_i}\sim\Gamma\left(a_0,b_0\right)\qquad \tau_{v_j}\sim\Gamma\left(c_0,d_0\right)$$

  - The Bayesian posterior model is given based on the prior assumptions of the model parameters.

$$p\left(\mathbf{U},\mathbf{V},\boldsymbol{\tau}_\mathbf{u},\boldsymbol{\tau}_\mathbf{v},\mathbf{Z}\mid\mathbf{S}\right)\propto p\left(\mathbf{U},\mathbf{V},\boldsymbol{\tau}_\mathbf{u},\boldsymbol{\tau}_\mathbf{v},\mathbf{Z},\mathbf{S}\right)$$
$$=\prod_{(i,j)\in\Omega}p\left(s_{ij}\mid\mathbf{u}_i^H\mathbf{v}_j,z_{ij}\right)\prod_{i=1}^{Q}p\left(\mathbf{u}_i\mid\tau_{u_i}\right)$$
$$\times\prod_{j=1}^{T}p\left(\mathbf{v}_j\mid\tau_{v_j}\right)\prod_{i=1}^{Q}p\left(\tau_{u_i}\right)\prod_{j=1}^{T}p\left(\tau_{v_j}\right)\prod_{(i,j)\in\Omega}p\left(z_{ij}\right)$$

WBI mitigation methodology

- Approximate variational Bayesian inference
  - It is difficult to solve such a complex posterior probability directly.
  - The variational Bayesian inference can be utilized to approximate the full posterior distribution.
  - General solution of variational Bayesian inference can be written as:

$$q_j^*\left(\theta_j\right)=\frac{\exp\left(E_{i\neq j}\left[\ln p\left(\theta,S\right)\right]\right)}{\int\exp\left(E_{i\neq j}\left[\ln p\left(\theta,S\right)\right]\right)d\theta_j}$$

- The approximate distribution and factorization results for the forward Bayesian posterior can be given as following

$$q\left(\mathbf{U},\mathbf{V},\boldsymbol{\tau}_{\mathbf{u}},\boldsymbol{\tau}_{\mathbf{v}},\mathbf{Z}\right)=\prod_{i=1}^{Q}q\left(\mathbf{u}_i\right)\prod_{j=1}^{T}q\left(\mathbf{v}_j\right)$$

$$\times\prod_{i=1}^{Q}q\left(\tau_{u_i}\right)\prod_{j=1}^{T}q\left(\tau_{v_j}\right)\prod_{ij}q\left(z_{ij}\right)$$

WBI mitigation methodology

- Alternating iteration until convergence

➢ Estimation of $q(\mathbf{u}_i)$ and $q(\tau_{u_i})$,with parameters $\boldsymbol{\Lambda}_{u_i},\boldsymbol{\mu}_{u_i},a_i,b_i$:

$$q(\mathbf{u}_i)=CN\left(\mathbf{u}_i\,|\,\boldsymbol{\mu}_{u_i},\boldsymbol{\Lambda}_{u_i}^{-1}\right)$$
$$q(\tau_{u_i})=\Gamma\left(\tau_{u_i}\,|\,a_i,b_i\right)$$

$$\boldsymbol{\Lambda}_{u_i}=E\left[\boldsymbol{\tau}_{u_i}\right]I+\sum_{j=1}^{T}E\left[z_{ij}^{-1}\right]E\left[\mathbf{v}_j\mathbf{v}_j^H\right]$$
$$\boldsymbol{\mu}_{u_i}=\boldsymbol{\Lambda}_{u_i}^{-1}\sum_{j=1}^{T}\mathbf{S}_{ij}^H E\left[z_{ij}^{-1}\right]E\left[\mathbf{v}_j\right]$$
$$a_i=a_0+r,b_i=b_0+E\left[\mathbf{u}_i^H\mathbf{u}_i\right]$$

➢ Estimation of $q(\mathbf{v}_j)$ and $q(\mathbf{v}_j)$,with parameters $\boldsymbol{\Lambda}_{v_j},\boldsymbol{\mu}_{v_j},c_j,d_j$;

$$q(\mathbf{v}_j)=CN\left(\mathbf{v}_j\,|\,\boldsymbol{\mu}_{v_j},\boldsymbol{\Lambda}_{v_j}^{-1}\right)$$
$$q(\tau_{v_j})=\Gamma\left(\tau_{v_j}\,|\,c_j,d_j\right)$$

$$\boldsymbol{\Lambda}_{v_j}=E\left[\boldsymbol{\tau}_{v_j}\right]I+\sum_{i=1}^{Q}E\left[z_{ij}^{-1}\right]E\left[\mathbf{u}_i\mathbf{u}_i^H\right]$$
$$\boldsymbol{\mu}_{v_j}=\boldsymbol{\Lambda}_{v_j}^{-1}\sum_{j=1}^{Q}\mathbf{S}_{ij}E\left[z_{ij}^{-1}\right]E\left[\mathbf{u}_i\right]$$
$$c_j=c_0+r,d_j=d_0+E\left[\mathbf{v}_j^H\mathbf{v}_j\right]$$

WBI mitigation methodology

- Substitute $q\left(z_{ij}\right)$ with $q\left(z_{ij}^{-1}\right)$, then estimate $q\left(z_{ij}^{-1}\right)$,with parameters $\boldsymbol{\mu}_{z_{ij}^{-1}}, \lambda_{z_{ij}^{-1}}$:

$$q\left(z_{ij}^{-1}\right) = \mathcal{IG}\left(z_{ij}^{-1} \mid \mu_{z_{ij}^{-1}}, \lambda_{z_{ij}^{-1}}\right) \Longleftarrow \quad \mu_{z_{ij}^{-1}} = \sqrt{\frac{1}{\lambda E\left[\left(STFT_{x_{ij}} - \mathbf{u}_i^H \mathbf{v}_j\right)^2\right]}}, \quad \lambda_{z_{ij}^{-1}} = \frac{2}{\lambda}$$

- Estimation of λ

$$\lambda = \frac{\sum_{j=1}^{T}\sum_{i=1}^{Q} E\left[z_{ij}\right]}{QT}$$

- Reconstruct interference and cancellation in time domain

$$\boxed{\hat{x}(k) = s(k) - ISTFT\left[\left(\mathbf{U}^*\right)^H \mathbf{V}^*\right]}$$

Experimental results

- Data description
  - C-band Sentinel-1 satellites of the European Space Agency (ESA)
  - Resolution : 5m × 20m (Rang × azimuth)

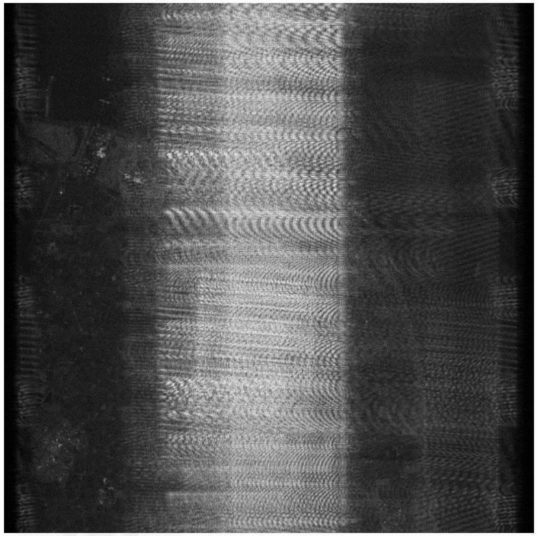

Azimuth

（a） original

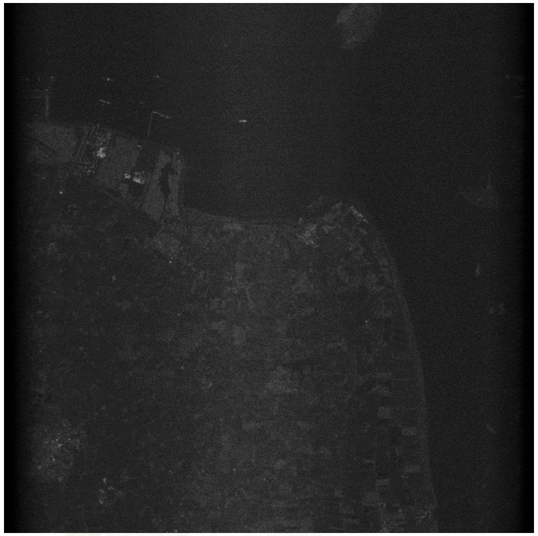

Azimuth

（b） GoDec

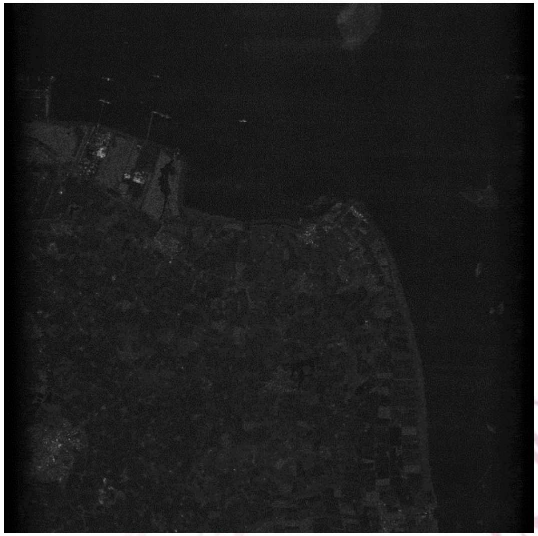

Azimuth

（c） proposed method

Experimental 1. The measured SAR data is acquired by the Sentinel-1A in VH polarization mode. The mitigation results shows that the imaging applying proposed method is better than that by GoDec.

Experimental results

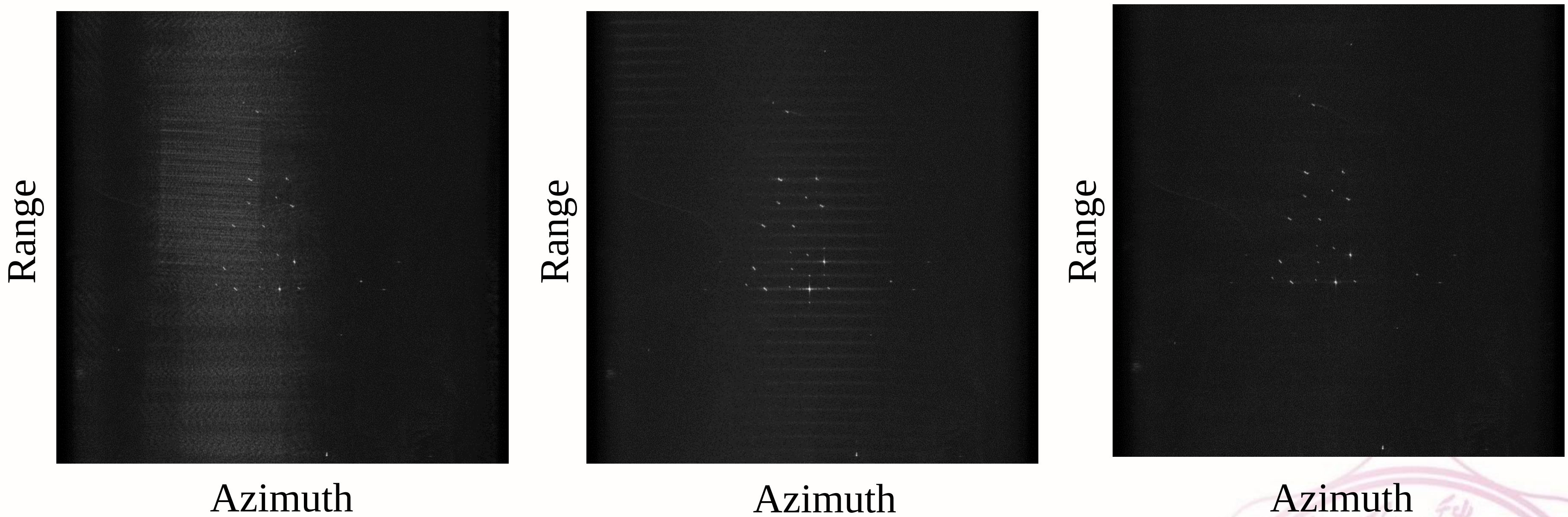

（a） original （b） GoDec （c） proposed method

Experimental 2. The measured SAR data is acquired by the Sentinel-1B in VH polarization mode. It shows that there is some residual interference in scene and ships are blurred by WBI after applying the GoDec. However, it can be seen that WBI is well mitigated and ships are well-focused after applying the proposed method.

Experimental results

- Quantitative analysis

$$MNR = 10\log_{10}\left(\frac{\frac{1}{N}\sum_{n=1}^{N}|I_n|^2}{\frac{1}{M}\sum_{m=1}^{M}|I_m|^2}\right)$$

A smaller MNR demonstrate the contrast of SAR image is stronger.

N and I_n represent the number of pixels of the weak scattering area and the corresponding pixel value; M and I_m represent the number of pixels of the strong scattering area and the corresponding pixel value.

Data \ Method	Original	GoDec	Proposed Method
Sentinel-1A VH	5.49dB	-5.87dB	-10.09dB
Sentinel-1B VV	-7.08dB	-12.41dB	-14.90dB

Conclusion remarks

- Innovation
  - Constructing a factorization model for recovery WBI.
  - Establish Bayesian model formulation , and use variational Bayesian inference for posterior probability estimation.
- Future research
  - Keeping find proper probability models for WBI and designing effective interference mitigation method in the future
  - Jamming and Anti-Jamming never ends

Reference

1. M. Tao, J. Su, Y. Huang, L. Wang, “Mitigation of Radio Frequency Interference in Synthetic Aperture Radar Data: Current Status and Future Trends,” MDPI Remote Sens. 11, 20, Oct. 2019, pp.2438. doi:10.3390/rs11202438.

2. M. Tao, F. Zhou, Z. Zhang, “Wideband Interference Mitigation in High-Resolution Airborne Synthetic Aperture Radar Data,” IEEE Trans. Geosci. Remote Sens. 54,1, Jan 2016, pp. 74–87. doi:10.1109/TGRS. 2015.2450754.

3. S. Zhang, M. Xing, R. Guo, L. Zhang, Z. Bao, “Interference Suppression Algorithm for SAR Based on Time–Frequency Transform,” IEEE Trans. Geosci. Remote Sens. 49, 10, Oct. 2011, pp.3765–3779. doi:10.1109/ TGRS.2011.2164409.

4. W. Fan, F. Zhou, M. Tao, X. Bai, P. Rong, S. Yang, T. Tian. “Interference Mitigation for Synthetic Aperture Radar Based on Deep Residual Network,” MDPI Remote Sens. 11, 14, Jul. 2019, pp.1654. doi:10.3390 /rs11141654.

Reference

5. J. Su, H. Tao, M. Tao, L. Wang, J. Xie, “Narrow-band Interference Suppression via RPCA-Based Signal Separation in Time-Frequency Domain,” IEEE J. Sel. Topics Appl. Earth Obs. Remote Sens. 10, 11, Aug. 2017, pp.5016–5025. doi:10.1109/ JSTARS.2017. 2727520.

6. Y. Huang, L. Zhang, “A Novel Tensor Technique for Simultaneous Narrowband and Wideband Interference Suppression on Single-Channel SAR System,” IEEE Trans. Geosci. Remote Sens. 57, 12, Aug.2019, pp. 9575–9588. doi:10.1109/ TGRS.2019. 2927764.

7. Q. Zhao, D. Meng, Z. Xu, W. Zuo, Y. Yan. “L1-Norm Low-Rank Matrix Factorization by Variational Bayesian Method,” IEEE Trans. Neural Netw. Learn Syst. 26, 4, Jan.2015, pp. 825–839. doi: 10.1109/TNNLS.2014. 2387376.

8. D. F. Andrews and C. L. Mallows, “Scale mixtures of normal distributions,” J. Roy. Statist. Soc., Ser. B (Methodological), 36, 1, 1974, pp. 99–102.

Thanks for your attentions!